Design and Performance Analysis of Nonlinearity Preprocessors in an Impulsive Noise Environment

Hyungkook Oh, *Student Member, IEEE*, and Haewoon Nam, *Senior Member, IEEE*

***Abstract*—This paper discusses a practical design of nonlinearity preprocessors to be used in a receiver for mitigating performance degradation in an impulsive noise environment. A simple method is proposed for a blanker and a soft limiter to calculate a blanking and a clipping threshold, respectively. In addition, to evaluate the bit error performance of a receiver with the proposed nonlinearity preprocessors, this paper introduces an approach using a periodic pulse train function and Fourier series. When a nonlinearity preprocessor is used, since the output samples show a truncated probability density function, it is generally difficult to evaluate the bit error performance of a receiver. Analytical and simulation results show that the thresholds computed by the proposed method are near optimal in terms of efficacy function and that the error performance of the proposed nonlinearity preprocessors matches well with that of the ideal design of nonlinearity preprocessors with optimal thresholds.**

***Index Terms*—Blanking and clipping non-linearities, impulsive noise, Middleton class A noise.**

I. Introduction

MOST existing digital communication systems are designed to perform optimally in an additive white Gaussian noise (AWGN) environment. However, there are some environments where transmitted signals are contaminated by impulsive noise or non-Gaussian noise. For example, in-vehicular communication network suffers from various types of noises from mechanical parts in a vehicle, power line communication needs to consider noises coming from appliance switching, and underwater communications are impaired by noises from ocean living creature [1]. Since the conventional receivers suffer a significant performance degradation due to an impulsive noise in such an environment, it is important, if possible, to design a simple and practical add-on block (or preprocessor) that avoids or mitigates the performance degradation while using the conventional receiver. Among the impulsive noise models, the Middleton class A noise model is often applied because noises expressed by this model match physical phenomena very well and it is also known as a good statistical model about an electromagnetic interference signal [2], [3].

Manuscript received November 22, 2014; revised November 17, 2015 and February 14, 2016; accepted March 25, 2016. Date of publication March 29, 2016; date of current version January 13, 2017. This work was supported by the research fund of the Signal Intelligence Research Center supervised by the Defense Acquisition Program Administration and the Agency for Defense Development of Korea. The review of this paper was coordinated by Dr. S. Sun.

The authors are with the Division of Electrical Engineering, Hanyang University, Ansan 426-791, South Korea (e-mail: hnam@hanyang.ac.kr).

Color versions of one or more of the figures in this paper are available online at http://ieeexplore.ieee.org.

Digital Object Identifier 10.1109/TVT.2016.2547889

The design of the optimal receiver in an impulsive noise environment is first discussed in [4], where the optimal receiver is constructed based on maximum likelihood (ML) method. However, due to the high complexity of its analytical form, the authors offer a locally optimum receiver with a simpler method called threshold detector to be used as a nonlinearity preprocessor. The threshold detector gives many researchers an intuition about the design of nonlinearity preprocessors. In [5], simple and practical nonlinearity preprocessors, i.e., a blanker and a soft limiter, are introduced. In particular, the blanker and the soft limiter are required to determine the optimal blanking and clipping thresholds, respectively, for the best performance. Also in [5], since the optimal threshold is numerically computed, the blanking or the clipping threshold may not be calculated on an on-demand basis in practical systems.

With regard to the design of a blanker, [6] and [7] considered to find the optimal blanking threshold in an orthogonal frequency-division multiplexing (OFDM) system by maximizing signal-to-noise ratio (SNR). However, the blanking threshold by this method is only valid for the case of Bernoulli–Gaussian random process, and the asymptotic performance analysis given in the paper is only correct when the number of symbols is very large. Reference [8] proposes an iterative interference cancellation for OFDM signal with a blanker to suppress intercarrier interference, but this scheme does not provide a simple expression for the blanking threshold.

Other nonlinearity preprocessors than a blanker and a soft limiter are proposed for performance improvement in OFDM systems. In [9], the Mengi–Haring iterative scheme with replacement-nulling scheme, which combines nonlinearity preprocessors of a soft limiter and a blanker is proposed, but the threshold is not optimized with criterion. A nonlinearity preprocessor called deep clipping is proposed in [10], where the deep clipping offers small threshold change in various environments and provides a higher output SNR than a blanker and a soft limiter. However, the threshold in [10] is also numerically computed.

To satisfy an on-demand basis for practical systems, a closed form of a clipping threshold is derived by using signal detection theory in the application of power line communications [11]. In addition, a threshold of a soft limiter based on a decision boundary evaluation is proposed in [12]; the threshold is optimal when the oversampling number is 2. However, the threshold is not guaranteed in case when the oversampling number is more than 2. In addition, a blanker with an adaptive blanking threshold based on SNR is proposed as a nonlinearity in [13], where the nonlinearity provides a quasi-optimal threshold and a simple form of threshold. However, since the computation of the

threshold is dependent on signal power and noise parameters, it is not assured that the threshold is clearly calculated in low SNR due to the fact that the SNR estimate is biased [14].

This paper first proposes a method to derive simple analytical equations for the quasi-optimal blanking and clipping thresholds for practical nonlinearity preprocessors such as a blanker and a soft limiter. These simple and neat expressions allow the receiver to calculate or update the blanking or the clipping threshold of the preprocessor on the fly when it is necessary, which may be an essential functionality for practical receivers. Furthermore, the proposed thresholds for a blanker and a soft limiter are simply calculated only by noise parameters to minimize error rate. Since the proposed thresholds depend on noise parameters that are generally estimated, the impact of noise parameter estimation errors on the performance is also investigated. Then, the bit error rate (BER) performance of the receivers with various practical nonlinearity preprocessors in an impulsive noise environment is given as closed forms. Unlike conventional receivers in an AWGN environment, the BER performance of a receiver with nonlinearity preprocessors in an impulsive noise environment is challenging to analyze due to the nonlinear block and the complex noise model. To the authors' best knowledge, no results have been reported as of the moment on closed forms of BER performance of a receiver with nonlinearity preprocessors, such as a blanker and a soft limiter, under impulsive noise such as Middleton class A noise. Note that, due to the discontinuity and a limited signal range by nonlinear blocks, the conventional method of BER performance analysis cannot be used. Thus, to analyze the BER performance of a receiver with nonlinearity preprocessors, a method using pulse train function with finite sample space of output is applied in this paper.

This paper is organized as follows. Section II briefly describes the system model and summarizes the property of the Middleton class A noise model, including the statistics required to solve signal detection problems. As a reference, Section III reviews the optimal receiver in [4]. Section IV introduces practical nonlinearity preprocessors under consideration and discusses simple expressions of quasi-optimal blanking and clipping thresholds for the preprocessors. In Section V, the BER performance of receivers with nonlinearity preprocessors is analyzed. In addition, simulation results are compared with the BER performance analysis in Section VI. Finally, Section VII summarizes the conclusions.

II. Noise and System Models

The probability density function (pdf) of an instantaneous amplitude of the noise is useful for the design of a receiver, as well as the performance evaluation [4]. Among various impulsive noise models, the Middleton class A noise model has been commonly used by many researchers since the model agrees well with physical phenomena [2]. The pdf of an instantaneous amplitude of Middleton class A noise is given as

$$f_Z(z)=\sum_{m=0}^{\infty}\frac{e^{-A}A^m}{m!}\frac{1}{\sqrt{2\pi\sigma_m^2}}e^{-\frac{z^2}{2\sigma_m^2}}=\left\langle\frac{1}{\sqrt{2\pi\sigma_m^2}}e^{-\frac{z^2}{2\sigma_m^2}}\right\rangle_m \tag{1}$$

where $\sigma_m^2=\sigma^2((m/A)+\Gamma/(1+\Gamma))$, A gives the mean impulsive order due to the fact that a Middleton class A noise is a Gaussian noise whose power depends on order m, and is called impulsive index, Γ is defined as the power ratio between Gaussian noise components and impulsive noise components, and σ^2 is the average power of the noise [2]. In addition, $\langle a_m(z)\rangle_m$ denotes the expectation of $a_m(z)$ distributed as a Poisson random variable with A. The parameter A is in the range from 0.01 to 1 in practice. The impulsiveness of the noise is characterized by the values of those parameters. The smaller the value of A is, the more impulsive the noise in the environment is. If the value of Γ is smaller, the noise is more impulsive. The pdf mainly consists of two parts: the term with $m=0$ and the other terms with $m\geq 1$, where each term is a weighted Gaussian pdf where the weight is determined by a Poisson pdf. The term with $m=0$ in (1) is the Gaussian noise component, whereas the terms with $m\geq 1$ correspond to the impulsive noise component, in which each term has a growing variance as m increases. Due to the fact that the variances of the terms with $m\geq 1$ are generally much larger than that of the term with $m=0$, the $m\geq 1$ part is regarded as the impulsive noise component.

Considering the aforementioned examples of communication channels with impulsive noise, this paper considers binary phase-shift keying (BPSK) system, where the received signal at the receiver can be written as

$$X(n)=s_i(n)+Z(n),\quad 1\leq n\leq N \tag{2}$$

where $Z(n)$ is a Middleton class A noise, N is the number of oversampling, and $s_i(t)$ is a transmitted BPSK symbol, where $i=1,\ 2$. During the symbol duration, the receiver takes N samples from the received signal, where the noise of each sample is assumed to have no correlation with the other samples [12], [15], whereas the signal samples have a constant value. Each BPSK sample at the receiver is expressed as

$$\begin{aligned} s_1(n)&=\sqrt{\frac{E_b}{N\sigma^2}},\qquad 1\leq n<N\\ s_2(n)&=-\sqrt{\frac{E_b}{N\sigma^2}},\quad 1\leq n<N \end{aligned} \tag{3}$$

where E_b and σ^2 are the bit energy and the average noise power, respectively.

III. Optimal Nonlinearity

After an optimal receiver based on ML is introduced, optimal nonlinearity with BPSK system is discussed here when the interfering noise is a Middleton class A noise. The optimal receiver is based on an ML detector. Using Bayesian rule, the optimal receiver, which is denoted by $\Lambda(X)$, is expressed as [4]

$$\Lambda(X)=\frac{f_Z(X-s_2)}{f_Z(X-s_1)}=\frac{\prod_{n=1}^{N}\left\langle\frac{1}{\sqrt{2\pi\sigma_m^2}}e^{-\frac{(x_n-s_{2n})^2}{2\sigma_m^2}}\right\rangle_m}{\prod_{n=1}^{N}\left\langle\frac{1}{\sqrt{2\pi\sigma_m^2}}e^{-\frac{(x_n-s_{1n})^2}{2\sigma_m^2}}\right\rangle_m}\underset{s_2}{\overset{s_1}{\lessgtr}}1 \tag{4}$$

where X is the received signal vector, $f_Z(z)$ is the Middleton class A pdf in (1), N is the number of samples within a symbol, and s_{1n} and s_{2n} are the binary symbols for the nth sample. Note that the optimal receiver is maximizing capacity through the receiver. The mathematical model based on ML in (4) cannot be further required to be simplified, since calculating threshold of nonlinearity cannot be derived from the mathematical model. Although (4) shows the lowest error rate in an impulsive noise environment, the optimal receiver is difficult, if possible at all, to construct in practice due to its high complexity. Moreover, it offers no intuition about how to make a practical design. Thus, optimal nonlinearity is discussed for practical design.

With the assumption of small received signals, Taylor series approximation can be applied to the pdf such that $f_Z(X - s_i)$ in (4) can be represented as

$$f_Z(X - s_i) = f_Z(X) - \sum_{j=1}^{N} \frac{\partial f_Z(X)}{\partial x_j} s_{ij} + \frac{1}{2} \sum_{j=1}^{N} \sum_{k=1}^{N} \frac{\partial^2 f_Z(X)}{\partial x_j \partial x_k} s_{ij} s_{ik} + \cdots \quad (5)$$

where X is a received signal vector that consists of N samples; s_i is a vector of transmitted BPSK symbol; x_j and s_{ij} are the jth element of X and s_i, respectively; and $i = 1, 2$. Since the first two terms are strongly dominant in (5) [16], it can be simplified as

$$f_Z(X - s_i) \approx f_Z(X) - \sum_{j=1}^{N} \frac{\partial f_Z(X)}{\partial x_j} s_{ij}. \quad (6)$$

Note that, due to Taylor series approximation, the complex equation in (4) is altered to a simple sum of a couple of calculable terms. Additionally, the multiplication in (4) is eliminated, making it possible to compute the analytic form of the local optimum receiver (LO receiver). It is also worth noting that small-signal assumption is reasonable since the negative impact of impulsive noise on the performance is severe in small received signals, requiring a new design of the receivers to mitigate the negative impact.

Substituting (6) into (4), the optimal receiver is approximated as

$$\Lambda(X) \approx \frac{f_Z(X) - \sum_{j=1}^{N} \frac{\partial f_Z(X)}{\partial x_j} s_{2j}}{f_Z(X) - \sum_{j=1}^{N} \frac{\partial f_Z(X)}{\partial x_j} s_{1j}} = \frac{1 - \sum_{j=1}^{N} s_{2j} \frac{d}{dx_j} \ln f_Z(X)}{1 - \sum_{j=1}^{N} s_{1j} \frac{d}{dx_j} \ln f_Z(X)} \underset{s_2}{\overset{s_1}{\lessgtr}} 1. \quad (7)$$

Since the denominator and the numerator in (7) are positive due to the small-signal assumption, the LO receiver, which is denoted by $g_{\mathrm{LO}}(X)$, is derived as [4]

$$g_{\mathrm{LO}}(X) = \sum_{i=1}^{N} (s_{1i} - s_{2i}) \frac{d}{dx_i} \ln f_Z(x_i) \underset{s_2}{\overset{s_1}{\lessgtr}} 0 \quad (8)$$

where $\ln(x)$ is the natural logarithm function evaluated at x, and d/dx_i denotes the differentiation with respect to x_i. The effect of each x_i is not affected by the other elements owing to the fact that the number of oversampling during one symbol duration is sufficiently low for practical systems [12]. This is the reason why x_i is independent from the other elements in X. In addition, it is important to note that the LO receiver in (8) is characterized by $(d/dx_i) \ln f_Z(x_i)$, which is called nonlinearity, followed by the conventional receiver. This indicates that a well-designed nonlinearity block can be used as a preprocessor along with the conventional receiver in an impulsive noise environment without redesigning a completely new receiver. This is the reason why the design and the performance evaluation of nonlinearity preprocessors are important and are the focus of this paper.

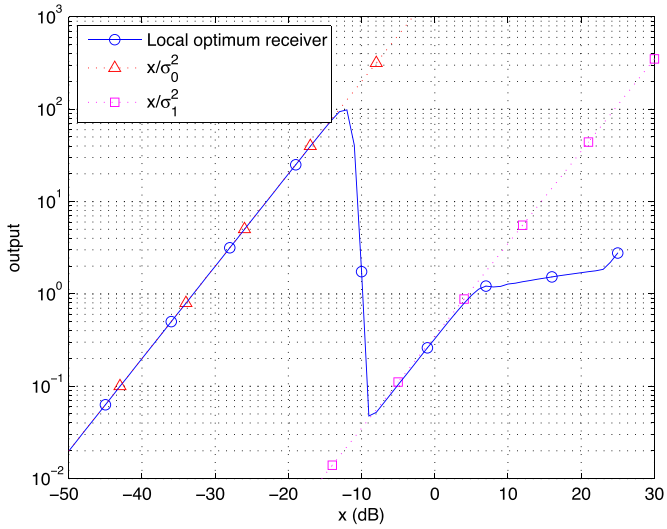

Fig. 1. Nonlinearity of the LO receiver in an environment of $A = 0.1$ and $\Gamma = 0.0005$.

The analytic form of the nonlinearity preprocessor of the LO receiver is given as

$$g_{\mathrm{LO}}(x) = \frac{d}{dx_i} \ln f_Z(x_i) = -\frac{f_Z'(x)}{f_Z(x)} = \frac{\left\langle \frac{1}{\sqrt{2\pi\sigma_m^2}} e^{-\frac{x^2}{2\sigma_m^2}} \frac{x}{\sigma_m^2} \right\rangle_m}{\left\langle \frac{1}{\sqrt{2\pi\sigma_m^2}} e^{-\frac{x^2}{2\sigma_m^2}} \right\rangle_m}. \quad (9)$$

Although this LO receiver is simpler than the optimal receiver in (4), it is still difficult to implement in practical systems due to the infinite sum in (9). It is possible, however, to get some intuitive hints from the input and output signals relationship of the LO receiver.

Fig. 1 illustrates the nonlinearity of the LO receiver in (9) in terms of input and output signals. It can be seen that the input signals with small amplitudes (less than -10 dB in Fig. 1), which are supposedly Gaussian noise components, are amplified by a constant gain (a linear curve between the input and the output). On the other hand, the nonlinearity of the LO receiver suppresses the input signals with large amplitudes (more than -10 dB in Fig. 1), which are presumably corrupted by impulsive noise, by which the impulsiveness can be reduced. In addition, Fig. 1 also shows that the nonlinearity in (9) can be tightly approximated by the two linear curves illustrated in the figure, where one is for Gaussian noise component and the other is for impulsive noise component (or non-Gaussian noise

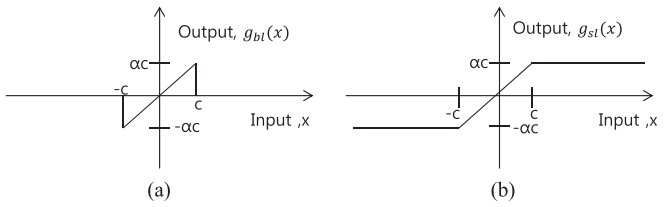

Fig. 2. Plotting the existing nonlinear blocks. (a) Blanker. (b) Soft limiter.

component). Those two linear curves can be characterized by their slopes, which are obtained as

$$g_{\mathrm{LO}}(x)|_{m=0} = \frac{\frac{e^{-A}A^0}{0!}\frac{1}{\sqrt{2\pi\sigma_0^2}}e^{-\frac{x^2}{2\sigma_0^2}}\frac{x}{\sigma_0^2}}{\frac{e^{-A}A^0}{0!}\frac{1}{\sqrt{2\pi\sigma_0^2}}e^{-\frac{x^2}{2\sigma_0^2}}} = \frac{x}{\sigma_0^2} \tag{10}$$

$$g_{\mathrm{LO}}(x)|_{m=1} = \frac{\frac{e^{-A}A^1}{1!}\frac{1}{\sqrt{2\pi\sigma_1^2}}e^{-\frac{x^2}{2\sigma_1^2}}\frac{x}{\sigma_1^2}}{\frac{e^{-A}A^1}{1!}\frac{1}{\sqrt{2\pi\sigma_1^2}}e^{-\frac{x^2}{2\sigma_1^2}}} = \frac{x}{\sigma_1^2}. \tag{11}$$

These observations suggest two design principles. First, the term with $m = 1$ is strongly dominant in the impulsive noise component ($A < 1$), which simplifies the analytical model of nonlinearity. A similar conclusion is also reported in [16]. Second, nonlinearity preprocessors can be designed and practically implemented based on the two linear curves and the threshold that separates the regions for these two curves. Since the SNR regions for those two linear curves are separated by a certain threshold, which is about -10 dB in the figure, it is also important to determine the threshold by a simple method.

IV. Practical Design of Nonlinearity Preprocessors

In [5], practical nonlinearity preprocessors, which are a blanker and a soft limiter that can be used in an impulsive noise environment, are discussed. Fig. 2 presents those nonlinearity preprocessors. Although those nonlinearity preprocessors are simple and practical, it is required for a blanker and a soft limiter to determine the blanking and clipping thresholds, which are denoted by c in the figure. In [5], the optimal c values are only obtained by numerical calculations of maximizing the efficacy function adopted in this paper, since the capacity or the BER dependent on oversampling number is too complex to obtain a closed form. However, for a practical design of those nonlinearity preprocessors, it is of paramount importance to find an easy and simple method to calculate the thresholds that are as close to optimal as possible.

Here, a simple analytic method of calculating the thresholds for nonlinearity preprocessors is proposed. In addition, we also investigate that the thresholds obtained by the proposed method are tightly close to the true optimal threshold values by performance comparisons.

A. Blanker

The nonlinearity of a blanker, i.e., $g_{bl}(x)$, is given as

$$g_{bl}(x, c_{bl}) = \begin{cases} \alpha x, & \|x| \le c_{bl} \\ 0, & \|x| > c_{bl} \end{cases} \tag{12}$$

where c_{bl} is the blocking threshold, and α is the gain of the blanker [5].

To test the optimality of nonlinearity preprocessors, the efficacy function is defined as [5]

$$\eta(g, f) = \frac{\left[\int_{-\infty}^{\infty} g(x, c) f_Z'(x)\, dx\right]^2}{\int_{-\infty}^{\infty} g^2(x, c) f_Z(x)\, dx} \tag{13}$$

where $g(x, c)$ is a nonlinearity, $f_Z(x)$ is the Middleton class A noise pdf, $f_Z'(x)$ is the derivative of $f_Z(x)$ with respect to x, and c is a blanking or a clipping threshold. Further derivation of (13) is written in the Appendix. Under mild regular condition, which is regularity condition in practice, [17] depicts that an error of a proposed method is minimized. The optimal threshold $c_{\mathrm{opt}-bl}$ that maximizes the efficacy function of the blanker is given as

$$c_{\mathrm{opt}-bl} = \arg\max_{c} \eta(g_{bl}, f). \tag{14}$$

Substituting (1) and (12) into (13), the efficacy function of a blanker is represented as

$$\eta(g_{bl}, f) = \frac{\left(\left\langle 2\alpha\left(\frac{1}{2}\mathrm{Erf}\left(\frac{c}{\sqrt{2\sigma_m^2}}\right) - \frac{c\cdot e^{-\frac{c^2}{2\sigma_m^2}}}{\sqrt{2\pi\sigma_m^2}}\right)\right\rangle_m\right)^2}{\left\langle 2\sigma_m^2\alpha^2\left(\frac{1}{2}\mathrm{Erf}\left(\frac{c}{\sqrt{2\sigma_m^2}}\right) - \frac{c\cdot e^{-\frac{c^2}{2\sigma_m^2}}}{\sqrt{2\pi\sigma_m^2}}\right)\right\rangle_m} \tag{15}$$

where $\mathrm{Erf}(x)$ is the error function evaluated at x. By substituting (15) into (14), $c_{\mathrm{opt}-bl}$ can be numerically calculated [5]. Note that, throughout this paper, the efficacy function serves as the reference method providing the optimal threshold, by which we evaluate the optimality of the thresholds obtained by the proposed methods.

Although (14) provides the optimal threshold, it is difficult to get the threshold from (15), because the $c_{\mathrm{opt}-bl}$ threshold is numerically updated. It is of critical importance to design a simple method of computing the threshold value for the nonlinearity to be used in practical systems. Since the LO receiver is optimal when the received signal is small, the proposed method is to design the nonlinearity preprocessor using the LO receiver as the reference. Motivated by the fact that the LO receiver is characterized by two linear curves, as discussed in Section III, and the LO receiver resembles a blanker if only the linear curve for Gaussian noise component is considered, the proposed method formulates a function, i.e., $g_{p-bl}(x)$, by taking only the minimum number of meaningful terms of the LO receiver in (9). The function is given as

$$g_{p-bl}(x) = \frac{e^{-A}\frac{1}{\sqrt{2\pi\sigma_0^2}}e^{-\frac{x^2}{2\sigma_0^2}}\frac{x}{\sigma_0^2}}{\sum_{m=0}^{1}\frac{e^{-A}A^m}{m!}\frac{1}{\sqrt{2\pi\sigma_m^2}}e^{-\frac{x^2}{2\sigma_m^2}}}. \tag{16}$$

Fig. 3 illustrates $g_{p-bl}(x)$ that shows the linear curve of x/σ_0^2 (applying a constant gain into the input signal) for small received signals, which is identical to the LO receiver. However, $g_{p-bl}(x)$ drops near the received signal amplitude of -10 dB, which means that the received signals with an amplitude larger

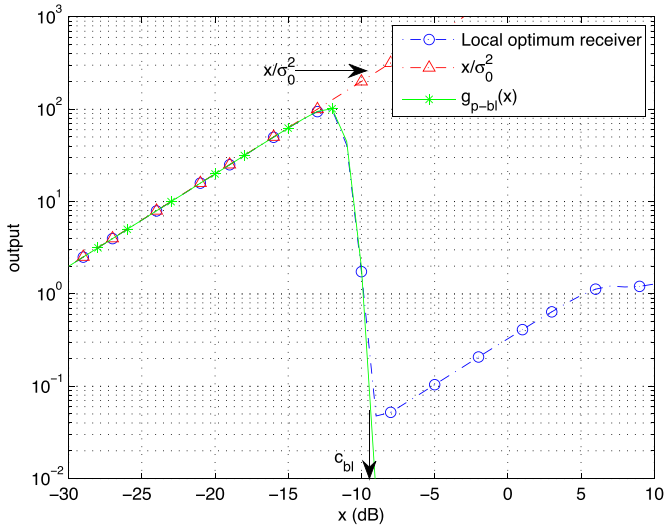

Fig. 3. Blocking threshold (c_{bl}) of a blanker by using x/σ_0^2 and $g_{p-bl}(x)$ in $A = 0.35$ and $\Gamma = 0.0005$.

than -10 dB are blocked (or zeroed out). Thus, it is shown in the figure that $g_{p-bl}(x)$ stems from the LO receiver, and it resembles a blanker, since the small received signal (Gaussian noise component) is amplified by the constant gain, whereas the large received signal (impulsive noise component) is zeroed out. For the design of a blanker, the blanking threshold needs to be determined.

In $g_{p-bl}(x)$, the blanking threshold c_{bl} is chosen as the cliff point of $g_{p-bl}(x)$, as shown in Fig. 3, which is approximated by the point where the function of the $m = 0$ term and that of the $m = 1$ term meet each other. The $m = 0$ term of the denominator in (16) is more dominant than the $m = 1$ term for small received signals (less than -10 dB in Fig. 3), whereas the $m = 1$ term is strongly dominant for large received signals (higher than -10 dB). Inspired by this approach, c_{bl} can be computed as

$$\alpha e^{-A}\frac{1}{\sqrt{2\pi\sigma_0^2}}e^{-\frac{c_{bl}^2}{2\sigma_0^2}} = \alpha A\cdot e^{-A}\frac{1}{\sqrt{2\pi\sigma_1^2}}e^{-\frac{c_{bl}^2}{2\sigma_1^2}} \tag{17}$$

from which the quasi-optimal blanking threshold is simply defined as

$$c_{bl} = \sqrt{\frac{\ln\left(\frac{1}{A}\sqrt{\frac{\sigma_1^2}{\sigma_0^2}}\right)}{\frac{1}{2\sigma_0^2}-\frac{1}{2\sigma_1^2}}} = \sqrt{\frac{\ln\left(\frac{1}{A}\sqrt{1+\frac{1}{A\Gamma}}\right)}{2\Gamma(1+A\Gamma)}} \tag{18}$$

where $\sigma_m^2 = ((m/A)+\Gamma/(1+\Gamma))$. Note that a blanker is effective in a highly impulsive noise environment (for instance, $A = 0.35$ and $\Gamma = 0.0005$).

To evaluate the optimality of the threshold value given by (18), Table I compares the threshold values obtained by the proposed method (c_{bl}) and the optimal threshold values computed by the efficacy function $(c_{\mathrm{opt}-bl})$ in (15) for various impulsive noise environments. As shown in the table, the difference between $c_{\mathrm{opt}-bl}$ and c_{bl} is negligible. Simulations also confirm that little difference in bit error performance is observed, which is shown in the following. Therefore, it is evident that the proposed method allows a simple and practical computation of the blanking threshold without noticeable performance loss.

In practical systems, the linear gain α is generally determined by the range of input signal amplitude to minimize the signal distortion when the signal passes through an analog-to-digital converter (ADC). Ignoring the effect of ADC and considering BPSK system, it is assumed that $\alpha = 1$ in (12) for simplicity.

B. Soft Limiter

The nonlinearity of a soft limiter, i.e., $g_{sl}(x)$, is given as

$$g_{sl}(x, c_{sl}) = \begin{cases} \alpha x, & |x| \le c_{sl} \\ \alpha c_{sl}, & x > c_{sl} \\ -\alpha c_{sl}, & x < -c_{sl} \end{cases} \tag{19}$$

where c_{sl} is a clipping threshold, where an input signal with a larger amplitude than c_{sl} is saturated to c_{sl}, and α is the gain of the soft limiter. Although the performance of a soft limiter depends on c_{sl}, a simple method calculating c_{sl} is not known yet. Only a numerical computation of c_{sl} is reported in [5].

Again, the efficacy function of a soft limiter is defined to serve as the reference. Substituting (1) and (19) into (13), the efficacy function of the soft limiter is given in (20), shown at the bottom of the page. Note that $\mathrm{Erfc}(x) = 1 - \mathrm{Erf}(x)$. Based on (20), the optimal clipping threshold of a soft limiter, i.e., $c_{\mathrm{opt}-sl}$, can be numerically computed as

$$c_{\mathrm{opt}-sl} = \arg\max_{c}\eta(g_{sl}, f). \tag{21}$$

However, since the numerical method is very complex, a simple method of calculating c_{sl} is proposed as follows.

Fig. 4 illustrates the nonlinearity of the LO receiver with a parameter set of $A = 0.5$ and $\Gamma = 0.1$ along with the linear curves x/σ_0^2 and x/σ_1^2. To determine clipping threshold with low computational complexity, we define a function $g_{p-sl}(x)$ by some meaningful terms in the LO receiver as

$$g_{p-sl}(x) = \frac{\sum_{m=0}^{1}\frac{e^{-A}A^m}{m!}\frac{1}{\sqrt{2\pi\sigma_m^2}}e^{-\frac{x^2}{2\sigma_m^2}}\frac{x}{\sigma_m^2}}{\sum_{m=0}^{1}\frac{e^{-A}A^m}{m!}\frac{1}{\sqrt{2\pi\sigma_m^2}}e^{-\frac{x^2}{2\sigma_m^2}}}. \tag{22}$$

$$\eta(g_{sl}, f) = \frac{\left(\left\langle 2\alpha\left(\frac{1}{2}\mathrm{Erf}\left(\frac{c}{\sqrt{2\sigma_m^2}}\right)-\frac{c\cdot e^{-\frac{c^2}{2\sigma_m^2}}}{\sqrt{2\pi\sigma_m^2}}\right)\right\rangle_m - 2\alpha\left\langle\frac{1}{\sqrt{2\pi\sigma_m^2}}e^{-\frac{c^2}{2\sigma_m^2}}\right\rangle_m\right)^2}{\left\langle 2\alpha^2\sigma_m^2\left(\frac{1}{2}\mathrm{Erf}\left(\frac{c}{\sqrt{2\sigma_m^2}}\right)-\frac{c\cdot e^{-\frac{c^2}{2\sigma_m^2}}}{\sqrt{2\pi\sigma_m^2}}\right)\right\rangle_m + 2\alpha^2\left\langle\mathrm{Erfc}\left(\frac{c}{\sqrt{2\sigma_m^2}}\right)\right\rangle_m} \tag{20}$$

TABLE I
OPTIMAL THRESHOLD ($c_{\mathrm{opt}-bl}$) BASED ON EFFICACY FUNCTION AND THE QUASI-OPTIMAL THRESHOLD (c_{bl}) BY THE PROPOSED METHOD

(A,Γ)	$(0.1,\ 5{\cdot}10^{-4})$	$(0.35,\ 5{\cdot}10^{-4})$	$(0.5,\ 5{\cdot}10^{-4})$	$(0.1,\ 5{\cdot}10^{-2})$	$(0.35,\ 5{\cdot}10^{-2})$	$(0.5,\ 5{\cdot}10^{-2})$
c_{opt-bl}	0.0851	0.0731	0.0693	0.6950	0.5747	0.5417
(η_{opt-bl})	(1781.1)	(1325.3)	(1101.8)	(17.5758)	(10.9274)	(8.2416)
c_{bl}	0.0852	0.0733	0.0696	0.6886	0.5464	0.4989
(η_{bl})	(1781.1)	(1325.3)	(1101.8)	(17.5746)	(10.8782)	(8.1323)

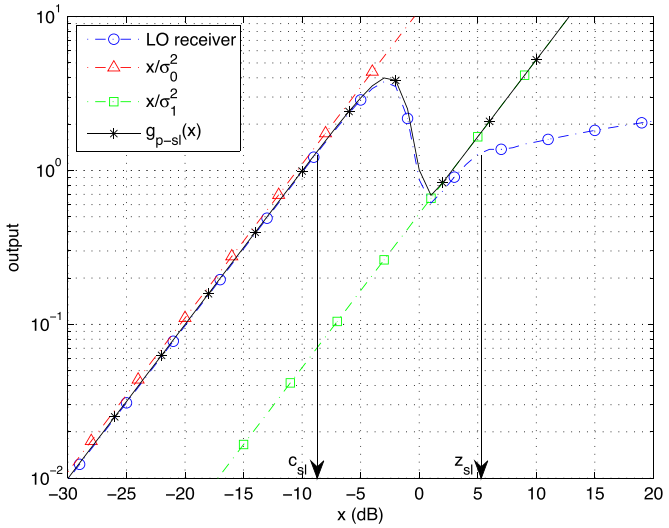

Fig. 4. Driving threshold (c_{sl}) of the soft limiter by using x/σ_0^2, x/σ_2^2, $g_{p-sl1}(x)$, and $g_{p-sl2}(x)$ in $A = 0.5$ and $\Gamma = 0.1$.

As shown in Fig. 4, $g_{p-sl}(x)$ is identical to the LO receiver when the input signal has a small amplitude (less than around 0 dB in the figure). When the input signal has a large amplitude (higher than 0 dB in the figure), however, $g_{p-sl}(x)$ follows the linear curve of $1/\sigma_1^2$ (a constant gain to the input signal), whereas the LO receiver shows a nearly flat (or slowly increasing) curve. Note that a soft limiter saturates (or clips) the input signal if the input signal has a higher amplitude than the clipping threshold. Thus, to determine the clipping threshold c_{sl}, the output value (the height of a soft limiter) of the LO receiver has to be analyzed. Since the LO receiver has a near-flat curve if the input signal is approximately larger than z_{sl}, we need to first calculate z_{sl}, from which the clipped value is obtained. Then, the clipped value is later mapped into the linear curve of x/σ_0^2 to determine c_{sl}. Based on the fact that the difference between $g_{p-sl}(x)$ and the LO receiver dominantly stems from the $m = 1$ and the $m = 2$ terms, the point that $g_{p-sl}(x)$ deviates from the LO receiver, which is denoted by z_{sl}, can be approximated by the following simple relationship between the $m = 1$ and the $m = 2$ terms:

$$\alpha \frac{e^{-A} A}{1!} \frac{1}{\sqrt{2\pi\sigma_1^2}} e^{-\frac{z_{sl}^2}{2\sigma_1^2}} = \alpha \frac{e^{-A} A^2}{2!} \frac{1}{\sqrt{2\pi\sigma_2^2}} e^{-\frac{z_{sl}^2}{2\sigma_2^2}} \tag{23}$$

which leads to z_{sl} as

$$z_{sl} = \sqrt{\frac{\frac{2}{A}\ln\left(\frac{\sigma_2^2}{\sigma_1^2}\right)}{\frac{1}{2\sigma_1^2} - \frac{1}{2\sigma_2^2}}}. \tag{24}$$

Since the threshold of a soft limiter has to be on x/σ_0^2, whereas z_{sl}/σ_1^2 is used for the height of a soft limiter, we can obtain

$$\frac{c_{sl}}{\sigma_0^2} = \frac{z_{sl}}{\sigma_1^2}. \tag{25}$$

Substituting (24) into (25), c_{sl} is given as

$$\begin{aligned} c_{sl} &= z_{sl}\frac{\sigma_0^2}{\sigma_1^2} = \frac{\sigma_0^2}{\sigma_1^2}\sqrt{\frac{\frac{2}{A}\ln\left(\frac{\sigma_2^2}{\sigma_1^2}\right)}{\frac{1}{2\sigma_1^2} - \frac{1}{2\sigma_2^2}}} \\ &= \Gamma\sqrt{\frac{4(2+A\Gamma)}{(1+\Gamma)(1+A\Gamma)}\ln\left(\frac{2+A\Gamma}{1+A\Gamma}\right)}. \end{aligned} \tag{26}$$

Table II evaluates the optimality of the quasi-optimal threshold given by the proposed method by comparing it with the optimal threshold maximizing the efficacy function. Unlike the case of a blanker, the threshold values by the proposed method for a soft limiter seem to be somewhat different from the optimal threshold values, but the corresponding efficacy values ($\eta_{\mathrm{opt}-sl}$ and η_{sl}) show that those thresholds computed by the proposed method indeed provide near-maximum efficacy values. It is also shown by simulations in the following that little difference in bit error performance is observed, which indicates that the proposed method achieves near-optimal performance while offering a simple way to calculate the threshold.

V. PERFORMANCE ANALYSIS

In an impulsive noise environment, a receiver takes N samples within a symbol, and those samples are combined for a symbol detection. The received signal can be modeled by a sum of random variables as $Y = \sum_{i=1}^{N} X_i$, where X_i is the random variable for the ith sample value. When BPSK modulation is used, the BER at the receiver is expressed as

$$\mathrm{BER} = \int_{-\infty}^{0} f_{Y|S=+1}(y)\, dy \tag{27}$$

where $f_{Y|S=+1}(y)$ is the pdf of y given that $S = +1$ is transmitted. Due to the nonlinear characteristics of the preprocessors and the oversampling performed at the receiver, the pdf $f_{Y|S=+1}(y)$ is generally difficult, if possible, to derive as an analytic expression. Thus, this section introduces a novel and generalized analytical approach based on a periodic pulse train and the Fourier series to derive the pdf and further analyze the BER performance of the nonlinearity preprocessors designed by the proposed methods.

TABLE II
OPTIMAL THRESHOLD ($c_{\mathrm{opt}-sl}$) MAXIMIZING THE EFFICACY FUNCTION AND THE QUASI-OPTIMAL THRESHOLD (c_{sl}) BY THE PROPOSED METHOD

(A,Γ)	$(0.1,\ 10^{-1})$	$(0.35,\ 10^{-1})$	$(0.5,\ 10^{-1})$	$(0.1,\ 10^{-3})$	$(0.35,\ 10^{-3})$	$(0.5,\ 10^{-3})$
c_{opt-sl}	0.1999	0.1397	0.1267	0.0157	0.0106	0.0088
(η_{opt-sl})	(7.2674)	(4.5733)	(3.6818)	(625.288)	(353.391)	(257.936)
c_{sl}	0.2232	0.2199	0.2179	0.0024	0.0024	0.0024
(η_{sl})	(7.2516)	(4.4139)	(3.5148)	(549.9774)	(333.6874)	(248.6727)

A. Conventional Receiver

As a reference, the BER performance of a conventional receiver is first analyzed. Note that the conventional receiver is not equipped with any nonlinear preprocessor. Since a sum of Middleton class A random variables becomes another Middleton class A random variable with different parameters [18], the pdf of a sum of Middleton class A noise samples is given as

$$f_{Y|S=+1}(y)=\sum_{m=0}^{\infty}\frac{e^{-N\cdot A}(N\cdot A)^m}{m!}\frac{1}{\sqrt{2\pi\sigma_{mN}^2}}e^{-\frac{(y-N\cdot u)^2}{2\sigma_{mN}^2}} \quad (28)$$

where $\sigma_{mN}^2=\sigma^2((m/A)+N\cdot\Gamma/(1+\Gamma))$.

Substituting (28) into (27), the BER of the conventional receiver is expressed as

$$\mathrm{BER}=\sum_{m=0}^{\infty}\frac{e^{-N\cdot A}(N\cdot A)^m}{m!}\frac{1}{2}\mathrm{Erfc}\left(\frac{N\cdot u}{\sqrt{2\sigma_{mN}^2}}\right). \quad (29)$$

B. Receiver With a Blanker

When a blanker is used as a preprocessor in an impulsive noise environment, the pdf of each output sample from a blanker is given as

$$f_X(x)=\begin{cases}\sum_{m=0}^{\infty}\frac{e^{-A}A^m}{m!}\frac{1}{2}\left(\mathrm{Erfc}\left(\frac{c-u}{\sqrt{2\sigma_m^2}}\right)+\mathrm{Erfc}\left(\frac{c+u}{\sqrt{2\sigma_m^2}}\right)\right)\\ \delta(x),\ x=0\\ \sum_{m=0}^{\infty}\frac{e^{-A}A^m}{m!}\frac{1}{\sqrt{2\pi\sigma_m^2}}e^{-\frac{(x-u)^2}{2\sigma_m^2}},\quad -c\le x\le c\end{cases} \quad (30)$$

which consists of a truncated pdf of a Middleton class A noise by the blanking threshold c and a Dirac delta function at $x=0$. The value of the delta function at $x=0$ corresponds to the probability that the input signal has a higher amplitude than c. $f_{Y|S=+1}(y)$ is computed by convolutions of $f_X(x)$ $N-1$ times owing to $Y=\sum_{i=1}^{N}X_i$, but multiple convolutions of the truncated pdf $f_X(x)$ are very difficult due to the discontinuity and the delta function in $f_X(x)$. The range of $f_Y(y)$ is $-Nc\le y\le Nc$, since it is obtained by $N-1$ convolutions of $f_X(x)$, where the range of $f_X(x)$ is $-c\le x\le c$. For calculating error rate, [19] takes a characteristic function and a Fourier transform and [20] uses Chernoff bound, while a receiver is by maximum *a posteriori* probability decoding. However, both [19] and [20] only computed the error rate numerically.

To avoid the computationally challenging task of multiple convolutions of truncated pdfs, we provide here a method of analyzing bit error performance using a periodic pulse train and Fourier series without the need to compute the multiple convolutions of $f_X(x)$. A similar approach is also used in [21], where a sum of Rayleigh random variables is computed based on the Fourier series and the pulse train function. In addition, [22] shows performance analysis of BPSK using a similar technique in Laplace noise. The BER performance of a receiver with a blanker is written using a pulse train function as

$$\begin{aligned}\mathrm{BER}&=\Pr(Y\le 0|S=+1)=\int_{-Nc}^{0}f_{Y|S=+1}(y)\,dy\\&=\int_{-\infty}^{\infty}f_{Y|S=+1}(y)\mathrm{PT}(y)\,dy\end{aligned} \quad (31)$$

where the periodic pulse train $\mathrm{PT}(y)$ and Fourier series of the pulse train are given as

$$\mathrm{PT}(x)=\begin{cases}1, & -T/2<x<0\\ 0, & 0\le x<T/2\end{cases}=\frac{1}{2}-\sum_{\substack{m=-\infty\\ m\ \mathrm{odd}}}^{\infty}C_m e^{jmwx} \quad (32)$$

where $C_m=1/jm\pi$, and T is the period of the pulse train. Substituting (32) into (31), the BER can be rewritten as

$$\begin{aligned}\mathrm{BER}&=\int_{-\infty}^{\infty}f_Y(y)\left(\frac{1}{2}-\sum_{\substack{m=-\infty\\ m\ \mathrm{odd}}}^{\infty}C_m e^{jmwy}\right)dy\\&=\frac{1}{2}-\sum_{\substack{m=-\infty\\ m\ \mathrm{odd}}}^{\infty}C_m\int_{-\infty}^{\infty}f_Y(y)e^{jmwy}\,dy\\&=\frac{1}{2}-\sum_{\substack{m=-\infty\\ m\ \mathrm{odd}}}^{\infty}C_m E[e^{jmwY}].\end{aligned} \quad (33)$$

By converting the negative region of the summation into positive, the BER equation can be simplified as

$$\begin{aligned}\mathrm{BER}&=\frac{1}{2}-\left(\sum_{\substack{m=1\\ m\ \mathrm{odd}}}^{\infty}C_m E[e^{jmwY}]+\sum_{\substack{m=-\infty\\ m\ \mathrm{odd}}}^{-1}C_m E[e^{jmwY}]\right)\\&=\frac{1}{2}-\left(\sum_{\substack{m=1\\ m\ \mathrm{odd}}}^{\infty}C_m E[e^{jmwY}]+\sum_{\substack{m=1\\ m\ \mathrm{odd}}}^{\infty}-C_m E[e^{j(-m)wY}]\right)\\&=\frac{1}{2}-\sum_{\substack{m=1\\ m\ \mathrm{odd}}}^{\infty}\frac{1}{jm\pi}\left(E[e^{jmwY}]-E[e^{-jmwY}]\right).\end{aligned} \quad (34)$$

Using $Y=\sum_{i=1}^{N} X_i$ and Euler's formula, the BER can be further simplified as

$$\begin{aligned}\text{BER} &= \frac{1}{2} - \sum_{\substack{m=1\\ m\ \text{odd}}}^{\infty} \frac{1}{jm\pi}\left(\prod_{i=1}^{N} E[e^{jmwx_i}] - \prod_{i=1}^{N} E[e^{-jmwx_i}]\right)\\ &= \frac{1}{2} - \sum_{\substack{m=1\\ m\ \text{odd}}}^{\infty} \frac{1}{jm\pi}\left(\prod_{i=1}^{N} A_{m,i}e^{j\theta_{m,i}} - \prod_{i=1}^{N} A_{m,i}e^{-j\theta_{m,i}}\right)\\ &= \frac{1}{2} - \sum_{\substack{m=1\\ m\ \text{odd}}}^{\infty} \frac{1}{jm\pi}\left(A_m e^{j\theta_m} - A_m e^{-j\theta_m}\right)\\ &= \frac{1}{2} - \frac{2}{\pi}\sum_{\substack{m=1\\ m\ \text{odd}}}^{\infty} \frac{A_m \sin(\theta_m)}{m} \end{aligned} \tag{35}$$

where

$$\begin{aligned} A_{m,i} &= \sqrt{E\left[\cos(mwx_i)\right]^2 + E\left[\sin(mwx_i)\right]^2}\\ \theta_{m,i} &= \arctan\frac{E\left[\sin(mwx_i)\right]}{E\left[\cos(mwx_i)\right]}\\ A_m &= \prod_{i=1}^{N} A_{m,i},\ \theta_m = \sum_{i=1}^{N}\theta_{m,i} \end{aligned} \tag{36}$$

$$E\left[\cos(mwx_i)\right] = \int_{-\infty}^{\infty} \cos(mwx_i) f_X(x_i)dx_i \tag{37a}$$

$$E\left[\sin(mwx_i)\right] = \int_{-\infty}^{\infty} \sin(mwx_i) f_X(x_i)dx_i \tag{37b}$$

where w is $(2\pi/T)$, $E[X]$ is an expectation of X, and $\sin(\cdot)$ and $\cos(\cdot)$ are trigonometric functions. It is worth noting that the integral operation in BER is altered to a summation in (35), due to the pulse train and Fourier series.

Substituting (30) into (37a), $E[\cos(mwx_i)]$ can be given as

$$\begin{aligned} E\left[\cos(mwx_i)\right] = \Bigg\langle \Bigg(&\frac{1}{2}\left\{\mathcal{C}_{F\cos}(a,b,h) - \mathcal{C}_{F\cos}(d,b,h)\right\}\\ &+\frac{1}{2}\text{Erfc}\left(\frac{c-u}{\sqrt{2\sigma_k^2}}\right) + \frac{1}{2}\text{Erfc}\left(\frac{c+u}{\sqrt{2\sigma_k^2}}\right)\Bigg)\Bigg\rangle_k \end{aligned} \tag{38}$$

where $\sigma_k^2 = (k/A+\Gamma)/(1+\Gamma)$, $g=-(m^2w^2\sigma_k^2)/2$, $a=(c-u)/\sqrt{2\sigma_k^2}$, $b=-(mw\sigma_k^2)/\sqrt{2\sigma_k^2}$, $h=umw$, and $d=-(c+u)/\sqrt{2\sigma_k^2}$. $\mathcal{C}_{F\cos}(a,b,h)$ in (38) is defined as

$$\mathcal{C}_{F\cos}(a,b,h) = \frac{1}{2}\text{Erf}(a+jb)e^{jh} + \frac{1}{2}\text{Erf}(a-jb)e^{-jh}. \tag{39}$$

For the error function of a complex number, an infinite series approximation in [23, 7.1.29] is given as

$$\begin{aligned} \text{Erf}(R+jI) = \text{Erf}(R) &+ \frac{2e^{-R^2}}{\pi}\sum_{n=1}^{\infty}\frac{2R\cdot e^{-\frac{n^2}{4}}}{n^2+4R^2} + \frac{e^{-R^2}}{\pi}\frac{1-e^{-j2RI}}{2R}\\ &- \frac{2e^{-R^2}}{\pi}e^{-j2RI}\sum_{n=1}^{\infty}\frac{e^{-\frac{n^2}{4}}}{n^2+4R^2}(2R\cosh(nI) - jn\sinh(nI)) \end{aligned} \tag{40}$$

where $R+jI$ is a complex number; and $\cosh(x)$ and $\sinh(x)$ are hyperbolic cosine and sine functions evaluated at x, respectively.

Using (40), (39) is rewritten as

$$\begin{aligned} \mathcal{C}_{F\cos}(a,b,h) = &\frac{e^{-a^2}}{2a\pi}\left\{\cos(h) - \cos(2ab-h)\right\}\\ &+ \frac{2e^{-a^2}}{\pi}\sum_{n=1}^{\infty}\frac{2a\cdot e^{-\frac{n^2}{4}}}{n^2+4a^2}\cos(h)\\ &+ \text{Erf}(a)\cos(h) - \frac{2e^{-a^2}}{\pi}\sum_{n=1}^{\infty}\frac{e^{-\frac{n^2}{4}}}{n^2+4a^2}\\ &\times\left\{2a\cosh(nb)\cos(2ab-h)\right.\\ &\left.+n\sinh(nb)\sin(2ab-h)\right\}. \end{aligned} \tag{41}$$

It is worth noting that $\mathcal{C}_{F\cos}(a,b,h)$ in (41) is not a complex number (no imaginary number), which can be understood by the fact that (39) is an addition of two complex conjugate terms. In addition, $\mathcal{C}_{F\cos}(d,b,h)$ in (38) can be also obtained by replacing a with d in (41). Substituting $\mathcal{C}_{F\cos}(a,b,h)$ and $\mathcal{C}_{F\cos}(d,b,h)$ into (38), $E[\cos(mwx_i)]$ is given as a closed form.

Similarly, substituting (30) into (37b), $E[\sin(mwx_i)]$ is obtained as

$$E[\sin(mwx_i)] = \left\langle \frac{e^g}{2}\left\{\mathcal{C}_{F\sin}(a,b,h) - \mathcal{C}_{F\sin}(d,b,h)\right\}\right\rangle_k \tag{42}$$

where $\mathcal{C}_{F\sin}(a,b,h)$ is given as

$$\mathcal{C}_{F\sin}(a,b,h) = \frac{1}{j2}\text{Erf}(a+jb)e^{jh} - \frac{1}{j2}\text{Erf}(a-jb)e^{-jh}. \tag{43}$$

Using (40), (43) is given as

$$\begin{aligned} \mathcal{C}_{F\sin}(a,b,h) = &\frac{e^{-a^2}}{2a\pi}\left(\sin(h) + \sin(2ab-h)\right)\\ &+\frac{2e^{-a^2}}{\pi}\sum_{n=1}^{\infty}\frac{2a\cdot e^{-\frac{n^2}{4}}}{n^2+4a^2}\sin(h) + \text{Erf}(a)\sin(h)\\ &+\frac{2e^{-a^2}}{\pi}\sum_{n=1}^{\infty}\frac{e^{-\frac{n^2}{4}}}{n^2+4a^2}\\ &\times\left(2a\cosh(nb)\sin(2ab-h)\right.\\ &\left.+n\sinh(nb)\cos(2ab-h)\right). \end{aligned} \tag{44}$$

Therefore, putting (44) into (42), $E[\sin(mwx_i)]$ is also obtained.

Substituting (38) and (42) into (36), the BER of a blanker is given as a closed form, by which the BER of a receiver with a blanker with any threshold value in an impulsive noise environment with arbitrary parameters can be analyzed.

C. Receiver With a Soft Limiter

The pdf of a received sample through a soft limiter is written as

$$f_X(x) = \begin{cases} \sum_{m=0}^{\infty}\frac{e^{-A}A^m}{m!}\frac{1}{2}\text{Erfc}\left(\frac{c-u}{\sqrt{2\sigma_m^2}}\right), & x=c\\ \sum_{m=0}^{\infty}\frac{e^{-A}A^m}{m!}\frac{1}{2}\text{Erfc}\left(\frac{c+u}{\sqrt{2\sigma_m^2}}\right), & x=-c\\ \sum_{m=0}^{\infty}\frac{e^{-A}A^m}{m!}\frac{1}{\sqrt{2\pi\sigma_m^2}}e^{-\frac{(x-u)^2}{2\sigma_m^2}}, & -c<x<c. \end{cases} \tag{45}$$

As aforementioned, it is very difficult to convolve $f_X(x)$ $N-1$ times due to the truncation and the Dirac delta functions in (45). However, due to the aforementioned $E[\cos(mwx_i)]$ and

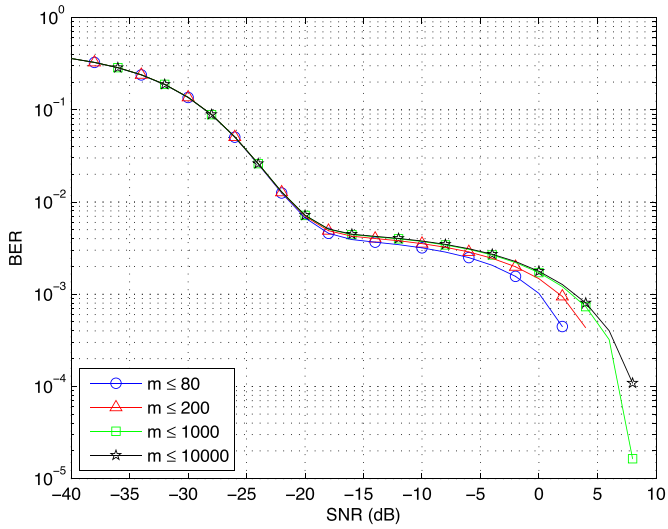

Fig. 5. BER of a soft limiter calculated by (35), (46), and (47) by various m when $A = 0.35$, $\Gamma = 0.0005$, and the number of signal sampling is 10.

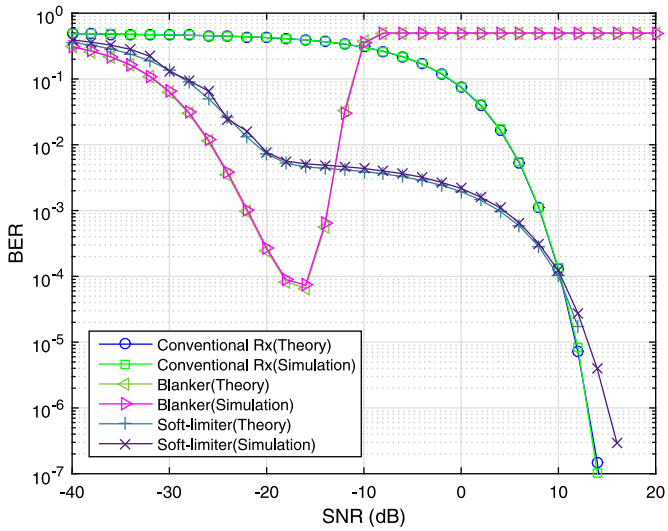

Fig. 6. Comparison of analytical result with simulation for a conventional receiver, a blanker with c_{bl}, and a soft limiter with c_{sl} when $A = 0.35$, $\Gamma = 0.0005$, and the number of signal sampling is 10.

$E[\sin(mwx_i)]$ calculations, substituting (45) into (37a) and (37b) allows

$$E\left[\cos(mwx_i)\right] = \left\langle \frac{e^g}{2}\left\{\mathcal{C}_{F\cos}(a,b,h) - \mathcal{C}_{F\cos}(d,b,h)\right\} + \frac{1}{2}\left\{\mathrm{Erfc}\left(\frac{c-u}{\sqrt{2\sigma_k^2}}\right) + \mathrm{Erfc}\left(\frac{c+u}{\sqrt{2\sigma_k^2}}\right)\right\}\cos(mwc)\right\rangle_k \tag{46}$$

$$E\left[\sin(mwx_i)\right] = \left\langle \frac{e^g}{2}\left\{\mathcal{C}_{F\sin}(a,b,h) - \mathcal{C}_{F\sin}(d,b,h)\right\} + \frac{1}{2}\left\{\mathrm{Erfc}\left(\frac{c-u}{\sqrt{2\sigma_k^2}}\right) - \mathrm{Erfc}\left(\frac{c+u}{\sqrt{2\sigma_k^2}}\right)\right\}\sin(mwc)\right\rangle_k . \tag{47}$$

The BER of a soft limiter is analyzed as a closed form by substituting (46) and (47) into (36).

D. Convergence of the Theoretical BER

Fig. 5 shows the impact of m on the BER performance of a soft limiter given by (35), (46), and (47). Due to its infinite summation of m in (35), the value of m needs to be truncated to a certain value so that the number of terms in the summation becomes finite to evaluate the BER performance in (35). As shown in Fig. 5, a very large number of m is required in order for the BER of a soft limiter to be accurate. The main reason of this slow convergence of BER equation in terms of m stems from the values of $\cos(mwc)$ and $\sin(mwc)$ in (46) and (47). The signs of $\cos(mwc)$ and $\sin(mwc)$ are alternating with respect to m, each with a different pattern, leading $E[\cos(mwx_i)]$ in (46) and $E[\sin(mwx_i)]$ in (47) to be fluctuating. This fluctuation of (46) and (47) eventually results in a slow convergence of BER equation of a soft limiter.

VI. Experimental Result

This section illustrates the performance of theoretical and empirical error rates of a blanker and a soft limiter with the proposed threshold and various thresholds for comparison. Section VI-A shows comparison of simulation results and theories of the proposed and optimal thresholds based on efficacy function. Section VI-B illustrates the impacts of noise parameters in the proposed thresholds based on badly estimated noise parameters. Section VI-C shows comparison of performance with the proposed thresholds and the other thresholds in other papers.

A. Performance of Nonlinearities With the Proposed and Optimal Thresholds

Numerous simulations are performed to evaluate the optimality of the design of the nonlinearity preprocessors discussed in Section IV by comparing an efficacy function and to verify the analysis for BER performance of a receiver with various nonlinearity preprocessors given in Section V. Several different noise parameter sets are selected for simulations to consider a strong and a moderate impulsive environment. In addition, the signal sampling is 10 ($N = 10$) for practical systems.

Figs. 6 and 7 plot the BER performance analysis and simulation results in a strong impulsive environment ($A = 0.35$ and $\Gamma = 0.0005$). The proposed quasi-optimal thresholds in (18) and (26) are used for the blanker and the soft limiter, respectively. The receiver with a blanker shows the lowest error rate in low SNR (less than -30 dB), which indicates that a blanker is an effective preprocessor in a highly impulsive environment. The BER of a blanker is lower than that of a soft limiter in low SNR due to the fact that the nonlinearity of a blanker more resembles the optimal nonlinearity. The BER of a soft limiter is lower than that of a blanker in high SNR, but there is no definite degradation of error rate between c_{bl} and c_{sl} in low SNR ($A = 0.35$ and $\Gamma = 0.05$). Based on Figs. 6 and 7, it is observed that the blanker is effective in a highly impulsive noise environment, whereas the soft limiter is dominant under moderate impulsive noise.

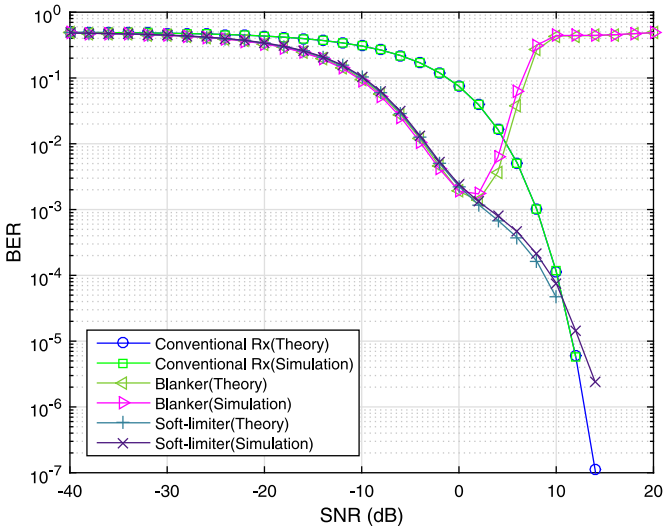

Fig. 7. Comparison of analytical result with simulation for a conventional receiver, a blanker with c_{bl}, and a soft limiter with c_{sl} when $A = 0.35$, $\Gamma = 0.05$, and the number of signal sampling is 10.

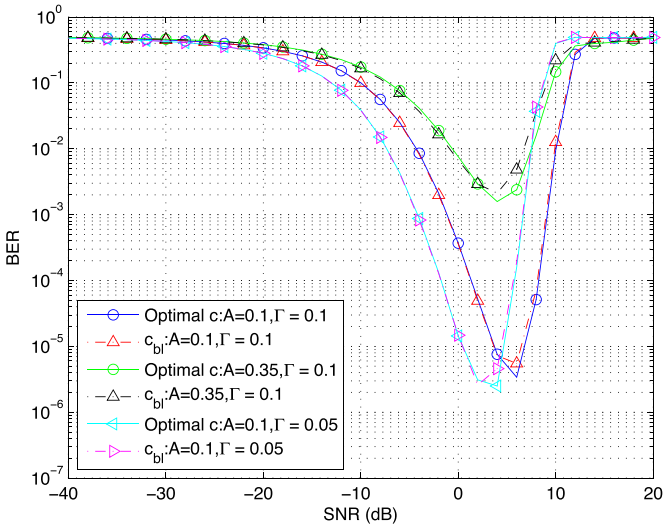

Fig. 8. BER performance of a blanker with the proposed threshold (c_{bl}) and the optimal threshold in $(A, \Gamma) = (0.1, 0.1)$, $(0.35, 0.1)$, $(0.1, 0.05)$, when the number of signal sampling is 10.

Fig. 8 depicts the BER performance of the proposed blanker for various noise parameter sets, such as $(A, \Gamma) = (0.1, 0.1)$, $(0.35, 0.1)$, $(0.1, 0.05)$. To evaluate the optimality of the blanking threshold c_{bl} given in (18), the BER performance of the blanker with the optimal threshold $c_{\mathrm{opt}-bl}$ obtained numerically by (14) is also plotted for comparison. As shown in the figure, no significant difference in BER performance is observed for all the noise parameter sets, indicating that the proposed method for computing blanking threshold is quasi-optimal.

Similarly, Fig. 9 illustrates the BER performance of the proposed soft limiter for various parameter sets, i.e., $(A, \Gamma) = (0.1, 0.05)$, $(0.35, 0.05)$, $(0.35, 0.0005)$, $(0.7, 0.05)$. The figure also shows that the proposed soft limiter with c_{sl} has almost identical BER performance to the soft limiter with the optimal clipping threshold $c_{\mathrm{opt}-sl}$ that is numerically calculated by (21)

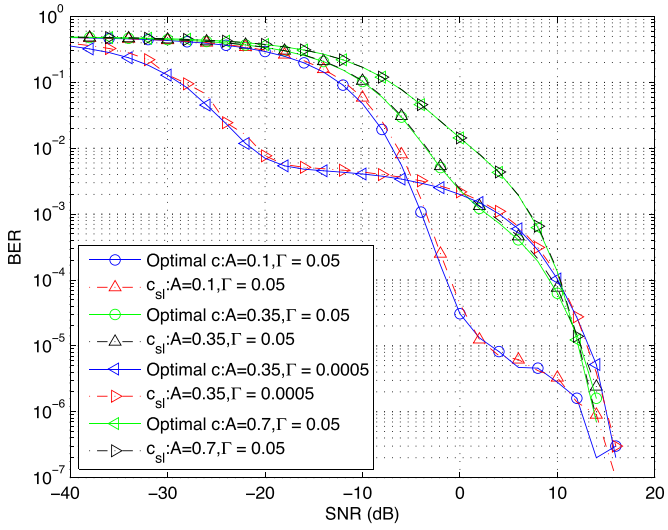

Fig. 9. BER performance of a soft limiter with the proposed threshold (c_{sl}) and the optimal threshold in $(A, \Gamma) = (0.1, 0.05)$, $(0.35, 0.05)$, $(0.35, 0.0005)$, $(0.7, 0.05)$, when the number of signal sampling is 10.

in various noise environments. Note that the BER of the soft limiter is close to the BER of the conventional receiver as A is close to 1, since the impulsive noise appears in the received signal more frequently as A increases.

B. Impact of Noise Parameter Estimation in the Proposed Thresholds

Since badly estimated noise parameters are one of the issues about a threshold of nonlinearity, simulation results based on the parameters will be illustrated. Then, the fact that a proposed calculation of a threshold is robust, while the noise parameters are badly estimated, is concluded. It is assumed that A and Γ are slightly changed during several data transmissions. Since the threshold of nonlinearity is computed by the estimated parameters, there may be some performance loss when the estimated parameters are not accurate. To see the impact of such a parameter estimation error on the performance, we have done numerous simulations as follows.

Reference [24] proposes an expectation–maximization algorithm for parameter estimation and [25] offers a method of empirical exceedance probability. In particular, [24] has shown estimation error of fractional mean square error (FMSE) < 0.05 with 100 samples per simulation, which is defined as

$$\mathrm{FMSE} = \left| \frac{a - \hat{a}}{a} \right|^2 \tag{48}$$

where a is a certain parameter value, and $\hat{a}$ is an estimated value. However, simulation results with 100 samples in [24] may be not adopted for estimation based on the small number of samples causing large FMSE. Thus, an estimated value with 3, 1/3, 10, and 1/10 times of original value, which causes large FMSE, is considered. Figs. 10 and 11 show the performance of a blanker and a soft limiter with various estimation errors. In addition, parameter sets of $(A, \Gamma) = (0.35, 0.0005)$ and $(0.1, 0.1)$, which are strongly impulsive, are assumed for a blanker and

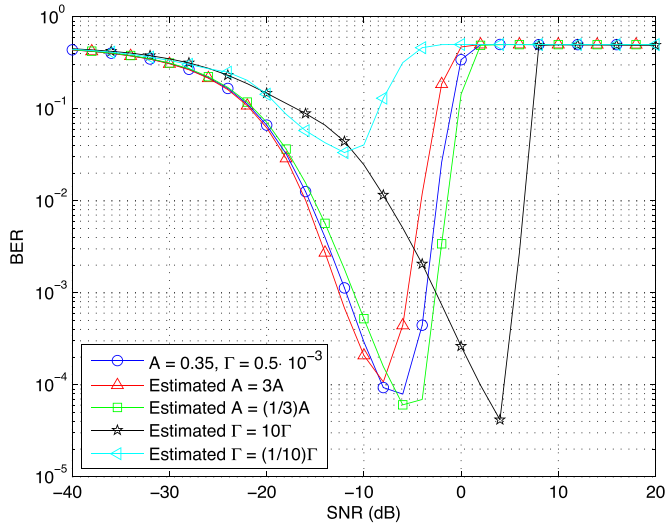

Fig. 10. BER of a blanker with a noise parameter estimation error in $A = 0.35$ and $\Gamma = 0.0005$.

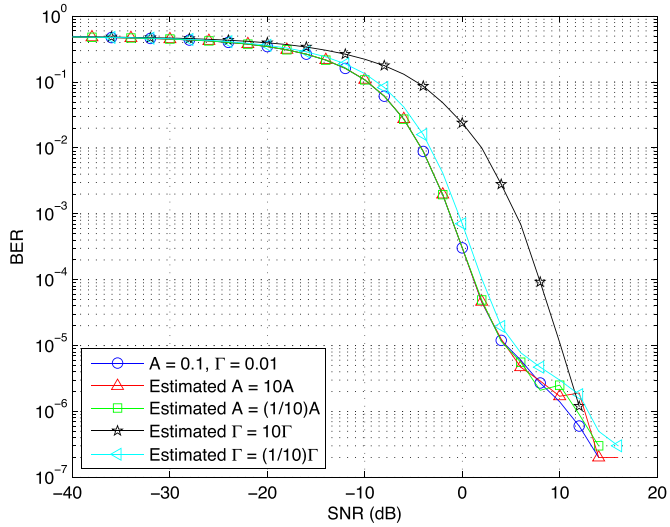

Fig. 11. BER of a soft limiter with a noise parameter estimation error in $A = 0.1$ and $\Gamma = 0.1$.

a soft limiter, respectively. In Figs. 10 and 11, there is little error rate degradation for BPSK system when A is incorrectly estimated, but badly estimated Γ causes performance degradation. However, there is little probability of estimated $\Gamma = 3\Gamma$ and estimated $\Gamma = 10\Gamma$ based on the fact that the FMSE of the estimated parameter is smaller than 0.05. Therefore, the proposed thresholds c_{bl} and c_{sl} are robust when noise parameters are badly estimated.

C. Performance Comparison Between the Proposed Threshold and the Other Thresholds

To confirm that nonlinearity with the proposed thresholds shows robust performance in low SNR, the performance of nonlinearity with the proposed threshold is compared with that of nonlinearities with the other thresholds in the literature. In BPSK system, under the assumption of a small A, [12] has

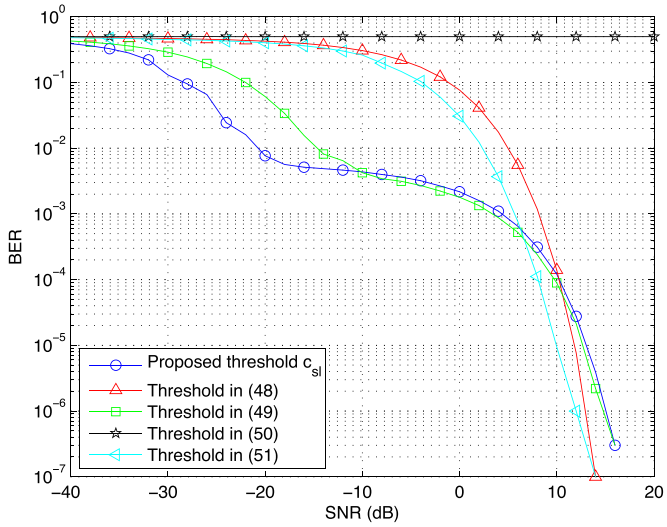

Fig. 12. BER of a soft limiter with various thresholds in $A = 0.35$ and $\Gamma = 0.5 \cdot 10^{-3}$ when the number of oversampling is 10.

proposed four thresholds based on decision boundary evaluation, by which the noise state is determined whether noise is Gaussian or impulsive noise. Based on this noise state and the threshold value, the received signal can be clipped or blocked. The proposed thresholds in [12] are represented as

$$\gamma_c^* = B + \sqrt{\frac{2\sigma_0^2\sigma_1^2}{\sigma_1^2 - \sigma_0^2} \ln\left(\frac{\sigma_1}{\sigma_0}\right)} \tag{49}$$

$$\gamma_s^* = B + z_0 \tag{50}$$

$$\gamma_l^* = B - z_0 + \frac{4B\sigma_0^2}{\sigma_1^2 - \sigma_0^2} \tag{51}$$

$$\gamma_m^* = B\frac{\sigma_0^2 + \sigma_1^2}{\sigma_1^2 - \sigma_0^2} \tag{52}$$

where $B = \sqrt{E_b/N\sigma^2}$, and $z_0 = \sqrt{(2\sigma_0^2\sigma_1^2)/(\sigma_1^2 - \sigma_0^2)\ln((\sigma_1 e^{-A})/(\sigma_0(1 - e^{-A})))}$.

Fig. 12 shows the BER performance of a soft limiter with the proposed threshold (c_{sl}) and the other thresholds in [12]. It is clearly observed that the proposed threshold gives the lowest error rate in low-SNR region (less than -10 dB). We can therefore claim that the proposed threshold allows more robust design of a soft limiter in low SNR.

VII. Conclusion

This paper has presented simple methods that obtain quasi-optimal thresholds of a blanker and a soft limiter. In addition, accurate performance analysis of nonlinearity proves the simulation results of the proposed scheme and the receiver with the optimal threshold. In addition, simulation results show not only that the blanker and the soft limiter are suitable in strong and moderate impulsive environments, respectively, but also that BERs of nonlinearities with the thresholds are close to those with the optimal thresholds in any impulsive environment.

APPENDIX

In [26] and [27], detection efficacy function as a measure of asymptotic detection performance, which is defined as

$$\eta(g,f)=\lim_{N\to\infty}\frac{\left(\frac{\partial E[Y_N|H_1]}{\partial s_{ij}}\right)^2}{N\mathrm{Var}[Y_N|H_0]} \tag{53}$$

is introduced, where $Y_N=\sum_{j=1}^{N}g(X_j)$, H_1 means that received samples include signal, and H_0 hypothesizes that noise samples are only observed. $\partial E[Y_N|H_1]/\partial s_{ij}$ in the numerator of (53) is computed as

$$\begin{aligned}\frac{\partial E[Y_N|H_1]}{\partial s_{ij}}&=\frac{\partial}{\partial s_{ij}}\int_{-\infty}^{\infty}\sum_{j=1}^{N}g(x_j)f(x_j-s_{ij})dx_j\\&\approx\sum_{j=1}^{N}\frac{\partial}{\partial s_{ij}}\int_{-\infty}^{\infty}g(x_j)\left(f(x_j)-\sum_{j=1}^{N}\frac{\partial f(x_j)}{\partial x_j}s_{ij}\right)dx_j.\end{aligned} \tag{54}$$

Since the partial derivative of $f(x_j)$ becomes 0, (54) is manipulated as

$$\begin{aligned}\frac{\partial E[Y_N|H_1]}{\partial s_{ij}}&\approx\sum_{j=1}^{N}\int_{-\infty}^{\infty}-g(x_j)\frac{\partial}{\partial s_{ij}}\left(\sum_{j=1}^{N}\frac{\partial f(x_j)}{\partial x_j}s_{ij}\right)dx_j\\&=N\int_{-\infty}^{\infty}-g(x_j)f'(x_j)dx_j.\end{aligned} \tag{55}$$

In addition, $\mathrm{Var}[Y_N|H_0]$ in the denominator of (53) is calculated as

$$\begin{aligned}\mathrm{Var}[Y_N|H_0]&=E[Y_N^2|H_0]-E[Y_N|H_0]^2\\&=\int_{-\infty}^{\infty}\left(\sum_{j=1}^{N}g(x_j)\right)^2f(x_j)dx_j\\&\quad-\left(\int_{-\infty}^{\infty}\sum_{j=1}^{N}g(x_j)f(x_j)dx_j\right)^2\\&=\sum_{j=1}^{N}\int_{-\infty}^{\infty}g(x_j)^2f(x_j)dx_j\\&\quad+\sum_{\substack{k=1,\\k\neq j}}^{N}\sum_{j=1}^{N}\int_{-\infty}^{\infty}g(x_k)g(x_j)f(x_j)dx_j\\&\quad-\left(\int_{-\infty}^{\infty}\sum_{j=1}^{N}g(x_j)f(x_j)dx_j\right)^2.\end{aligned} \tag{56}$$

Due to the fact that $g(x_j)$ and $f(x_j)$ are odd and even functions, respectively, the second and third terms of (56) are equal to 0. Thus, (56) is obtained as

$$\mathrm{Var}[Y_N|H_0]=N\int_{-\infty}^{\infty}g(x_j)^2f(x_j)dx_j. \tag{57}$$

Therefore, substituting (55) and (57) into (53), (53) is obtained as

$$\begin{aligned}\eta(g,f)&=\lim_{N\to\infty}\frac{\left(N\int_{-\infty}^{\infty}-g(x_j)f'(x_j)dx_j\right)^2}{N^2\int_{-\infty}^{\infty}g(x_j)^2f(x_j)dx_j}\\&=\frac{\left(\int_{-\infty}^{\infty}g(x_j)f'(x_j)dx_j\right)^2}{\int_{-\infty}^{\infty}g(x_j)^2f(x_j)dx_j}.\end{aligned} \tag{58}$$

REFERENCES

[1] Y. Yabuuchi *et al.*, "Low rate and high reliable modulation schemes for in-vehicle power line communications," in *Proc. IEEE ISPLC*, Apr. 2011, pp. 249–254.

[2] D. Middleton, "Statistical–physical models of electromagnetic interference," *IEEE Trans. Electromagn. Compat.*, vol. EMC-19, no. 3, pp. 106–127, Aug. 1977.

[3] D. Middleton, "Non-Gaussian noise models in signal processing for telecommunications: New methods and results for class A and class B noise models," *IEEE Trans. Inf. Theory*, vol. 45, no. 4, pp. 1129–1149, May 1999.

[4] A. Spaulding and D. Middleton, "Optimum reception in an impulsive interference environment—Parts I: Coherent detection," *IEEE Trans. Commun.*, vol. COM-25, no. 9, pp. 910–923, Sep. 1977.

[5] K. S. Vastola, "Threshold detection in narrow-band non-Gaussian noise," *IEEE Trans. Commun.*, vol. COM-32, no. 2, pp. 134–139, Feb. 1984.

[6] S. V. Zhidkov, "Performance analysis and optimization of OFDM receiver with blanking nonlinearity in impulsive noise environment," *IEEE Trans. Veh. Technol.*, vol. 55, no. 1, pp. 234–242, Jan. 2006.

[7] E. Alsusa and K. M. Rabie, "Dynamic peak-based threshold estimation method for mitigating impulsive noise in power-line communication systems," *IEEE Trans. Power Del.*, vol. 28, no. 4, pp. 2201–2208, Oct. 2013.

[8] C. Yih, "Iterative interference cancellation for OFDM signals with blanking nonlinearity in impulsive noise channels," *IEEE Trans. Signal Process.*, vol. 19, no. 3, pp. 147–150, Mar. 2012.

[9] V. N. Papilaya and A. J. H. Vinck, "Improving performance of the MH-iterative IN mitigation scheme in PLC systems," *IEEE Trans. Power Del.*, vol. 30, no. 1, pp. 138–143, Feb. 2015.

[10] F. H. Juwono, Q. Guo, D. Huang, and K. P. Wong, "Deep clipping for impulsive noise mitigation in OFDM-based power-line communications," *IEEE Trans. Power Del.*, vol. 29, no. 3, pp. 1335–1343, Jun. 2014.

[11] G. Ndo, P. Siohan, and M.-H. Hamon, "Adaptive noise mitigation in impulsive environment: Application to power-line communications," *IEEE Trans. Power Del.*, vol. 25, no. 2, pp. 647–656, Apr. 2010.

[12] K. A. Saaifan and W. Henkel, "Decision boundary evaluation of optimum and suboptimum detectors in class-A interference," *IEEE Trans. Commun.*, vol. 61, no. 1, pp. 197–205, Jan. 2013.

[13] H. Oh, H. Nam, and S. Park, "Adaptive threshold blanker in an impulsive noise environment," *IEEE Trans. Electromagn. Compat.*, vol. 56, no. 5, pp. 1045–1052, Sep. 2014.

[14] J. Astola and Y. Neuvo, "SNR estimation techniques for low SNR signals," in *Proc. 15th Int. Symp. WPMC*, Sep. 2012, pp. 276–280.

[15] A. D. Spaulding, "Amplitude and time statistics of urban manmade noise," in *Proc. Int. Commun. Conf.*, 1971, pp. 8–13.

[16] L. A. Berry, "Understanding Middleton's canonical formula for class A noise," *IEEE Trans. Electromagn. Compat.*, vol. EMC-23, no. 4, pp. 337–344, Nov. 1981.

[17] S. M. Kay, *Fundamentals of Statistical Signal Processing, Volume I: Estimation Theory*. Upper Saddler River, NJ, USA: Prentice-Hall, 1993.

[18] Y. Matsumoto, K. Gotoh, and K. Wiklundh, "Band-limitation effect on statistical properties of class-A interference," in *Proc. EMCEUROPE*, Sep. 2008, pp. 1–5.

[19] G. A. Tsihrinzis and C. L. Nikias, "Performance of optimum and suboptimum receivers in the presence of impulsive noise modelled as an alpha-stable process," *IEEE Trans. Commun.*, vol. 43, no. 2–4, pp. 904–914, Feb.–Apr. 1995.

[20] J. Haring and A. J. H. Vinck, "Performance bounds for optimum and suboptimum reception under class-A impulsive noise," *IEEE Trans. Commun.*, vol. 50, no. 7, pp. 1130–1136, Jul. 2002.

[21] N. C. Beaulieu, "An infinite series for the computation of the complementary probability distribution function of a sum of independent random variables and its application to the sum of Rayleigh random variables," *IEEE Trans. Commun.*, vol. 38, no. 9, pp. 1463–1474, Sep. 1990.

[22] S. Jiang and N. C. Beaulieu, "Precise BER computation for binary data detection in bandlimited white Laplace noise," *IEEE Trans. Commun.*, vol. 59, no. 6, pp. 1570–1579, Jun. 2011.

[23] M. Abramowitz and I. A. Stegun, *Handbook of Mathematical Functions With Formulas, Graphs, and Mathematical Tables*. New York, NY, USA: Dover, 1972.
[24] S. M. Zabin and H. V. Poor, "Efficient estimation of class A noise parameter via the EM algorithm," *IEEE Trans. Inf. Theory*, vol. 37, no. 1, pp. 60–72, Jan. 1991.
[25] D. Middleton, "Procedures for determining the parameters of the first-order canonical models of class A and class B electromagnetic interference," *IEEE Trans. Electromagn. Compat.*, vol. EMC-21, no. 3, pp. 190–208, Aug. 1979.
[26] J. W. Modestino and A. Y. Ningo, "Detection of weak signals in narrowband non-Gaussian noise," *IEEE Trans. Inf. Theory*, vol. IT-25, no. 5, pp. 592–600, Sep. 1979.
[27] B. Aazhang and H. V. Poor, "An analysis of nonlinear direct-sequence correlators," *IEEE Trans. Commun.*, vol. 37, no. 7, pp. 723–731, Jul. 1989.

Hyungkook Oh (S'16) received the B.S. degree in electronics and communication engineering in 2012 from Hanyang University, Ansan, South Korea, where he is currently working toward the Ph.D. degree.

His research interests include impulsive noise parameter estimation, communication system design in an impulsive noise environment, and multi-input–multi-output system design, as well as cooperative diversity.

Mr. Oh has received numerous scholarships, such as a Korean government scholarship for undergraduate study and an M.S. and Ph.D. degree scholarship.

Haewoon Nam (S'99–M'07–SM'10) received the B.S. degree from Hanyang University, Seoul, South Korea; the M.S. degree from Seoul National University; and the Ph.D. degree in electrical and computer engineering from the University of Texas at Austin, Austin, TX, USA.

From 1999 to 2002, he was with Samsung Electronics, Suwon, South Korea, where he was engaged in the design and development of Code Division Multiple Access and Global System for Mobile Communications (GSM)/General Packet Radio Service baseband modem processors. In the Summer of 2003, he was with the IBM Thomas J. Watson Research Center, Yorktown Heights, NY, USA, where he performed extensive radio channel measurements and analysis at 60 GHz. In the fall of 2005, he was with the Wireless Mobile System Group, Freescale Semiconductor, Austin, where he was engaged in the design and test of the Worldwide Interoperability for Microwave Access (WiMAX) medium access control layer. His industry experience also includes work with Samsung Advanced Institute of Technology, Kiheung, South Korea, where he participated in the simulation of multi-input–multi-output systems for the Third-Generation Partnership Project (3GPP) Long-Term Evolution (LTE) standard. In October 2006, he joined the Mobile Devices Technology Office, Motorola, Inc., Austin, where he was involved in algorithm design and development for the 3GPP LTE mobile systems, including modeling of 3GPP LTE modem processor. Later in 2010, he was with Apple Inc., Cupertino, CA, USA, where he worked on research and development of next-generation smart mobile systems. Since March 2011, he has been with the Department of Electronics and Communication Engineering, Hanyang University, Ansan, South Korea, where he is currently an Associate Professor.

Dr. Nam received the Korean government overseas scholarship for his doctoral studies in the field of electrical engineering.